High-wave-vector spin waves in ultrathin Co films on W(110)

M. Etzkorn,[1,*] P. S. Anil Kumar,[1,2] W. Tang,[1] Y. Zhang,[1] and J. Kirschner[1]
[1]*Max-Planck-Institut für Mikrostrukturphysik, Weinberg 2, D-06120 Halle, Germany*
[2]*Indian Institute of Science, 560 012 Bangalore, India*
(Received 27 July 2005; revised manuscript received 27 September 2005; published 16 November 2005)

We present an experimental study of high-wave-vector spin waves in 8 monolayer (ML) thick hexagonal closed-packed (hcp) Co films performed by spin-polarized electron energy loss spectroscopy (SPEELS). Using inelastic electron scattering, we were able to follow the spin wave dispersion up to the surface Brillouin zone boundary ($\bar{K}$), i.e., up to a wave-vector transfer of 1.64 Å^{-1}. The spin wave dispersion was found to agree surprisingly well with the dispersion relation of a surface spin wave calculated by a nearest-neighbor Heisenberg model. From this description, we obtain a value for the product of the exchange coupling constant (J) and the magnetic moment (S) of $JS=14.8\pm1$ meV. This value, within the error bar, is identical to our results obtained on thin fcc Co films on Cu(001). We also find that the spin wave features measured by SPEELS at high-wave-vectors are strongly broadened. This is in agreement with expectations from nonadiabatic theoretical descriptions in which the broadening is ascribed to a strong damping of these high-wave-vectors spin waves by Stoner excitations. Similar to the observations in previously studied systems, we also observe a strong dependence of the measured spin wave intensities on the kinetic energy of the incident electrons (E_{kin}). Highest spin wave intensities were found for low kinetic energies ($E_{\mathrm{kin}}<10$ eV).

DOI: 10.1103/PhysRevB.72.184420 PACS number(s): 75.30.Ds, 75.50.Cc, 75.70.Ak, 75.70.Rf

Spin waves in confined magnetic structures is a topic of growing interest.[1] Experimental studies of spin waves exclusively in such systems focus on the low-wave-vector regime, i.e., with wavelengths of at least some hundreds of Ångstrom. In fact, no established experimental technique has proven to be able to detect spin wave signals from ultrathin films and surfaces for wavelengths of the order of atomic lattice distances. These are, however, of fundamental interest because one may obtain information of magnetic properties on the atomic scale.

It has been recently demonstrated that by using spin-polarized electron energy loss spectroscopy (SPEELS) one is able to study high-wave-vector spin waves in ultrathin films.[2–4] Inelastic electron scattering provides both the necessary energy and momentum transfer, as well as a high surface sensitivity. So far, we have used this technique to study high-wave-vector spin waves in ultrathin fcc Co films grown on Cu(001),[4] as well as in different crystalline structures of Fe on Cu(001) and on W(110).[5–7] In the case of Fe, we found large differences in the spin wave properties measured on different crystalline structures stabilized on different substrates.[6,7] Here, we report on measurements performed on 8 ML thin hexagonal closed-pack (hcp) Co films grown on W(110). The results are compared to studies on 8 ML fcc Co grown on Cu(001). It is particularly interesting to compare these two crystalline structures because both phases can be found in bulk Co crystals. Bulk Co undergoes a martensitic phase transition from the low-temperature hcp to the high-temperature fcc phase at 690 K under ambient pressure.[8] When grown as thin films on a proper substrate, however, both crystalline structures can be stabilized under similar conditions. This allows a direct comparison of the magnetic properties at the same temperature. As will be discussed in the following, we found similar spin wave properties in these two systems.

The experiments have been preformed in a UHV chamber with a base pressure below 5×10^{-11} mbar. The W(110) single crystal was cleaned by a well-established cleaning procedure.[9] The crystal was repeatedly heated up to about 1600 K in 5×10^{-8} mbar O_2-atmosphere and subsequently flashed to temperatures larger than 2200 K (as determined by a pyrometer) to remove the oxygen from the surface. If C contaminations were found on the surface by auger electron spectroscopy after heating, the sample was heated in O_2 atmosphere again. Co was deposited by molecular beam epitaxy. The first ML was deposited shortly after the W heat treatment at substrate temperatures of approximately 600 K. The additional 7 ML have been deposited about 60 min after flashing so that the sample temperature was close to room temperature. This procedure is known to prevent the film from growing as islands and to improve the film quality.[10] Co films above the submonolayer regime grow on W(110) in a layer-by-layer fashion in a hcp structure with a (0001)-surface.[11–13] The hcp stacking was confirmed up to the twelfth ML.[10] The Co $[11\bar{2}0]$ direction is oriented parallel to the W[001] axis.[10] The large lattice misfit along this direction leads to the formation of a superstructure in which about five Co lattice spacings correspond to four W lattice spacings.[10] The resulting superstructure was followed in low energy electron diffraction (LEED) investigations up to the eighth ML.[11] Considering the above-mentioned ratio of five over four, the Co lattice is on average compressed by about 1% in the W [001] direction compared to its bulk lattice. Due to the deviations from bulk hcp Co and the shape anisotropy, the magnetic easy axis in thin Co films on W(110) lies in the film plane along the $[1\bar{1}00]$ direction.[11]

The Co film thickness was calibrated by the monolayer period oscillations in medium energy electron diffraction measured during the growth at a substrate temperature of 100 K, since the oscillations are known to be more pro-

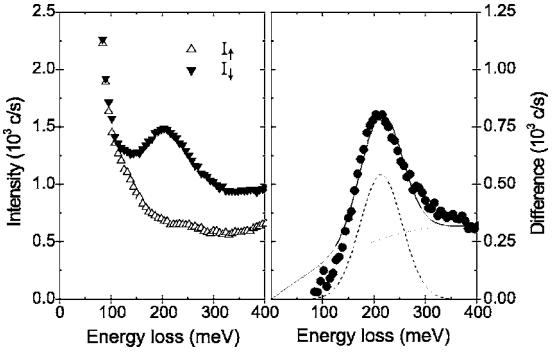

FIG. 1. The left panel shows SPEEL spectra of $I_\uparrow$ (△) and $I_\downarrow$ (▼) measured for a wave vector transfer of 0.88 Å^{-1} on an 8 ML Co film. The spectra are corrected for the incomplete polarization of the incident electron beam. In the right panel, the difference $I_\downarrow$-$I_\uparrow$ (●) is plotted. The solid line shows a fit to the difference, consisting of a Gaussian peak for the spin wave and a background, both are also shown separately as dashed and dotted lines, respectively. The spectra were measured with primary energy E_{kin}=4 eV, θ_0=80°, and an energy resolution of ΔE=40 meV.

nounced at this temperature.[10] The errors in the thickness calibration result mainly from the fluctuations of the Co source. The uncertainty is below 10% of the film thickness as crosschecked by the absolute signal of the Kerr ellipticity measured *in situ* on each Co film. The analysis of the Kerr measurements also reveals that the magnetization of the films is still fully saturated at remanence. This is a necessary condition to obtain the highest sensitivity to magnetic scattering in the SPEELS experiments. For the SPEELS measurements, the scattering plane was chosen to lie along the $(11\bar{2}0)$ direction, perpendicular to the magnetic easy axis. In the SPEELS experiments on hcp Co, we therefore probe spin wave properties along the $\bar{\Gamma}$-$\bar{K}$ direction in reciprocal space.

For the experiments we use a recently developed high-performance SPEEL spectrometer.[14] The spin-polarized electron beam is created from a strained GaAs photocathode with a polarization of $P=0.71\pm0.1$.[15,16] In the experiment, the spin of the incident electron beam can be switched from the parallel to the antiparallel direction with respect to the sample magnetization. In the following, $I_\uparrow$ ($I_\downarrow$) denotes the intensity of the scattered beam with incident spin parallel (antiparallel) to the spin of a majority electron inside the solid. The wave-vector transfer *parallel* to the sample surface is given by the scattering geometry: $\Delta K_\parallel = k_f \sin(\theta_0 - \theta) - k_i \sin(\theta)$. Here, k_f and k_i are the magnitude of the wave vector of the scattered and the incident electrons, and θ_0 and θ are the angles between the incident and the outgoing, and between the incident beam and the sample normal, respectively.

Figure 1 shows a representative example of SPEEL spectra measured on 8 ML Co on W(110). For this measurement we chose $\Delta K_\parallel = 0.88$ Å^{-1}. These spectra and all the following ones are corrected for the incomplete polarization of the incident electron beam. In Fig. 1 (right panel) a pronounced loss feature is clearly visible in $I_\downarrow$ (▼) at about 215 meV loss energy which is absent in $I_\uparrow$ (△). The loss peak results from inelastic scattering of electrons via the excitation of spin waves. As has been discussed in Ref. 4, the spin selective excitation process results from the fact that the spin angular momentum is conserved in the scattering process and that the excitation of a spin wave reduces the magnetization of the sample. This spin selective excitation can be used to distinguish spin wave excitations from other excitations. The spin selectivity can be exploited by calculating the difference of the two spectra recorded for the two possible orientations of the spin of the incident electron. The resulting difference spectrum is shown in Fig. 1 (left panel). We can fit this difference spectrum by a Gaussian for the spin wave peak and a background for electron hole pair excitations.

The measured spectra show that the spin wave peak is strongly broadened. The peak width is not determined by the finite resolution of the spectrometer but it is intrinsic. For the spectra shown in Fig. 1, the full width at half maximum (FWHM) of the spin wave peak corrected for the energy resolution of the spectrometer is 89±11 meV. We observed similar effects of an intrinsic width of the spin wave peaks in all other systems investigated so far.[4–7] The large intrinsic width of the spin wave peaks indicates strong damping of these excitations. As discussed in the literature, such a strong damping is expected for these high-wave-vector spin waves due to the efficient decay of spin waves into Stoner excitations,[17–19] i.e., electron hole pair excitations having opposite spin. The background visible in the spectra in Fig. 1 is caused by such electron hole pair excitations. The measured spin wave intensity in the $I_\downarrow$ spectrum is relatively strong. It is about 500 counts per second or 1% of the intensity of the elastic peak. This high intensity allows rather short data acquisition times. The spectra shown in Fig. 1, for example, were recorded in about 30 min.

We found that the measured spin wave intensity depends strongly on the kinetic energy of the incident electrons. We have chosen E_{kin}=4 eV and θ_0=80° for most measurements because at these conditions we observed the high-spin-wave intensity. For E_{kin}=4 eV the largest accessible wave vector transfer in our experimental set up is about 1 Å^{-1}. For larger wave vector transfers, the scattering conditions were changed to E_{kin}=25 eV and θ_0=90°. To illustrate the influence of the kinetic energy of the incident electrons, spectra measured at similar wave vector transfers but with E_{kin}=4 and 25 eV are shown in Fig. 2. The spectra in the upper panel [(a), (b)] were measured at $\Delta K_\parallel = 1.00$ Å^{-1} and with E_{kin}=4 eV at θ_0=80° and the spectra in the lower panel were obtained at $\Delta K_\parallel = 1.12$ Å^{-1} using E_{kin}=25 eV and θ_0=90°, respectively. Strong changes of the measured spectra are obvious. For the spectra measured with E_{kin}=25 eV, the most prominent loss features are vibrational excitations of small amounts of adsorbates present at the surface. These are clearly distinguishable from loss features caused by spin waves due to the missing spin selectivity in the excitation process, i.e., they appear in the intensity of both spin channels. The loss features at about 130 and 240 meV result from vibrational excitations of hydrogen and CO, respectively.[20] This has been confirmed for both in additional adsorption studies. The amount of adsorbates present at the surface can be estimated to be less than 10% coverage, as determined from these adsorption studies. The two spectra shown in Fig. 2 were recorded on two different samples identically prepared. At the

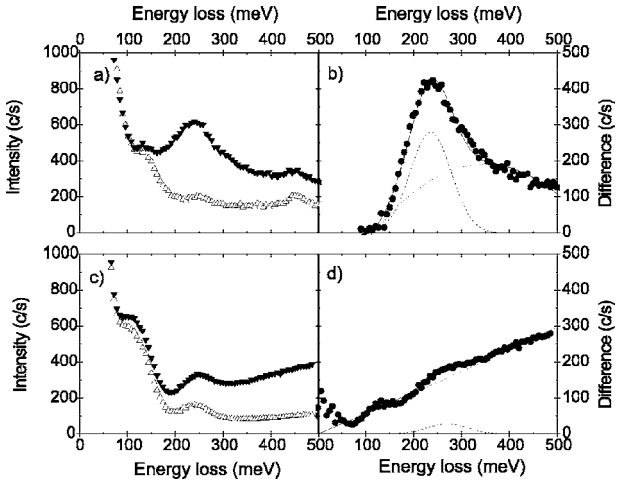

FIG. 2. SPEEL spectra and differences measured at $E_{\mathrm{kin}}=4$ eV, $\theta_0=80°$ (a,b), and $E_{\mathrm{kin}}=25$ eV, $\theta_0=90°$ (c,d) on 8 ML hcp Co. The spectra in the upper (lower) panel were measured with $\Delta K_{\parallel}=1.00$ Å^{-1} ($\Delta K_{\parallel}=1.12$ Å^{-1}). The total counting time for each data point in (a) and (c) was 10 and 50 s, respectively. The features in (a) and (c) around 130 and 240 meV are due to adsorbates, as discussed in the text. In the difference spectra, the fits and the separate contribution of spin wave and background are shown. The energy resolution in these scans was $\Delta E=40$ meV.

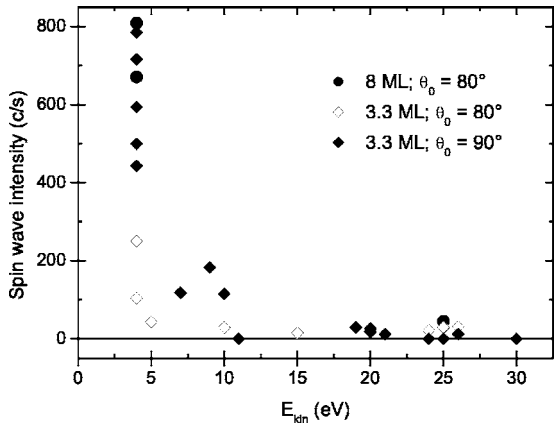

FIG. 3. The spin wave intensity as a function of different kinetic energies of the incident electrons measured by SPEELS. All points were measured for $\Delta K_{\parallel}=0.88$ Å^{-1}.

end of both measurements, the two films were about 4 h old. Thus, the higher intensities of the vibrational excitations measured with $E_{\mathrm{kin}}=25$ eV [Fig. 2(c)] is mainly caused by an enhanced cross section for these vibrational excitations at this kinetic energy. This increased intensity of the vibrational excitations has been constantly observed in all measurements using $E_{\mathrm{kin}}=25$ eV. In the $I_{\downarrow}$ spectrum shown in the lower panel of Fig. 2, the spin wave peak is located in the high-energy shoulder of the CO peak. This makes it difficult to see the spin wave loss directly in the spectrum. By exploiting the spin selectivity in the excitation process, it is, however, still possible to determine the spin wave energy in the difference spectrum shown in Fig. 2(d). Compared to Figs. 2(a) and 2(b), the spin wave loss peak is shifted from 235 meV to 265 meV loss energy because of the higher wave vector transfer involved. The spin wave intensity in Fig. 2(d) is reduced by more than an order of magnitude compared to the difference spectrum in Fig. 2(b). This is due partially to the higher-wave-vector transfer involved.[21] The largest effect, however, results from the dependence of the measured spin wave intensity on E_{kin}. We will discuss this point in more detail in the next paragraph. In addition, we find that for different values of E_{kin}, the background of electron hole pair excitations changes drastically. This is clearly visible in the spectra shown in Fig. 2.

We have investigated the dependence of the spin wave intensity on E_{kin} in more detail. We measured the spin wave intensity for a fixed-wave-vector transfer of $\Delta K_{\parallel}=0.88$ Å^{-1} as a function of E_{kin} for two scattering geometries ($\theta_0=80°$ and 90°) and two different Co film thicknesses (3.3 and 8 ML). The result is shown in Fig. 3. In general, we found high spin-wave-intensities only for small E_{kin}, below about 10 eV. These findings are very similar to the results obtained on Co and Fe films grown on Cu(001).[5,7] Since all three systems show a very similar dependence, qualitatively as well as quantitatively, this enhanced intensity seems to be a rather general effect. One should note that the spin wave intensity measured in the experiment depends on the cross section in the scattering process as well as on the transmission function of the spectrometer. The latter dependence is difficult to take into account, because it depends on the potentials applied to the spectrometer (about 40 different potentials). The settings of these potentials will be optimized before each measurement and therefore will differ from scan to scan. We attribute the scatter of the data mainly to this effect. The dependence of the spin wave cross section in an electron-scattering event on E_{kin} is an issue under investigation. In general, one would expect that the probability of an exchange-scattering event that is necessary to excite a spin wave, reduces with higher energy of the incident electrons.[22] The details of the scattering event are, however, not understood at the moment.

In addition, we find a strong dependence of the spin wave intensity on the scattering geometry and the wave vector transfer investigated. Thus, to allow comparison between different spectra, all measurements presented here were performed using only two different primary energies and two different θ_0.

One of the most important physical properties of spin waves is the dependence of their energy on the wave vector, i.e., the spin wave dispersion. Using SPEELS we were able to measure the spin wave dispersion over a wide-wave vector range. The result of the measurements on 8 ML hcp Co on W(110) are shown in Fig. 4 as solid squares. To allow comparison between the dispersions of hcp and fcc Co, we have also included the dispersion measured on 8 ML fcc Co on Cu(001) (○). The vertical dotted lines mark the surface Brillouin zone boundaries for the two crystalline structures. One can see that the spin wave energies are very similar in both systems for small-wave-vector transfers. At higher wave-vector transfers close to the surface Brillouin zone boundary of hcp Co, the spin wave energies in hcp Co become much larger than in fcc Co. For the wave vector range shown in Fig. 4, the spin wave energy is determined by the exchange interaction and all other contributions can be neglected.[23] To

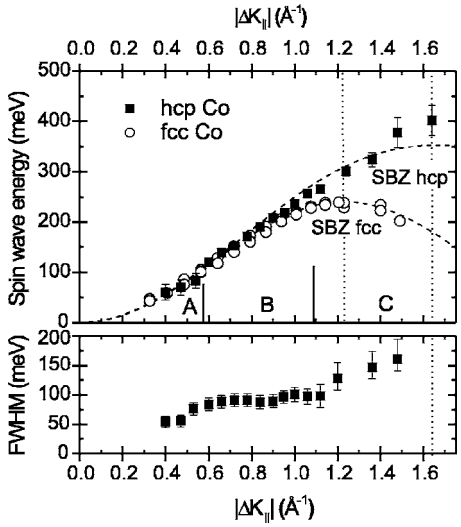

FIG. 4. Spin wave dispersion for 8 ML hcp Co on W(110) (■) and 8 ML fcc Co on Cu(001) (○) measured by SPEELS. The dashed lines are the dispersion relations for an acoustic surface spin wave mode calculated using a nearest-neighbor Heisenberg model (see text for details). The dotted lines mark the surface Brillouin zone boundaries for the two crystals. In regions A, B, and C, the SPEEL spectra on hcp Co were obtained using $E_{kin}=4$ eV, $\theta_0=80°$, and $\Delta E\approx 25$ meV (for A); $E_{kin}=4$ eV, $\theta_0=80°$, and $\Delta E\approx 40$ meV (for B), and $E_{kin}=25$ eV, $\theta_0=90°$, and $\Delta E\approx 40$ meV (for C). In the lower panel, the full width at the half maximum of the spin wave peak is shown. The width is corrected for the finite energy resolution of the spectrometer. The width for the peak at 1.64 $Å^{-1}$ could not be determined accurately and is not included in the graph.

describe the effect of the exchange interaction we use the Heisenberg model $H=-\Sigma_{ij}J_{ij}\mathbf{S}_i\cdot\mathbf{S}_j$. Here, J_{ij} is the exchange coupling constant between the magnetic moments $\mathbf{S}_i$ and $\mathbf{S}_j$. In the following discussion, we consider only nearest-neighbor interaction. The values for J and $\mathbf{S}$ are assumed to be independent of the position, i.e., to be identical at the surface, interface, and in the bulk. We have calculated the dispersion relation of the acoustic surface spin wave mode within this model and fitted it to our measured data.[24] The black dashed curves in Fig. 4 show the results of these fits.

The agreement to the experimental data is surprisingly good, considering the simplicity of the model and the fact that the geometrical shape of the dispersion is purely determined by the atomic arrangement in the crystal. The only fitting parameter is the product of JS, which defines the energy amplitude of the dispersion. The resulting value of JS for hcp Co is $JS=14.8\pm1$ meV. The measurements on fcc Co resulted in a value of $JS=15\pm1$ meV.[4] Within the experimental error we thus find the same value of JS for both crystalline structures. Hence, we are able to explain the differences in the measured dispersions purely by the different crystallographic directions measured in the two cases, while the exchange interaction remains similar in both Co phases. Very similar values for JS for Co arranged in different crystallographic lattices are in agreement with observations made by Brillouin light scattering (BLS) measurements, which were performed on thick (100 nm) Co films. In these experiments, practically no changes in the stiffness constant D for different Co lattices[25] was observed. Note that in the nearest-neighbor Heisenberg model $D=4JSa_0^2$. Using this relation, the values of JS found by BLS are 18.5 ± 0.6 meV for fcc and 17.3 ± 1.4 meV for hcp Co films, somewhat higher than the value measured in our experiments. One should, however, note that in the BLS experiments spin waves with several hundred times smaller wave vectors were probed.

The only experimental technique, that is able to study spin waves with similar wave vectors as SPEELS, is inelastic neutron scattering (INS). One INS study has been published on spin wave measurements with wave-vector transfers up to 0.8 $Å^{-1}$ on hcp Co.[26] The Co single crystal mass which was used in the INS experiments was about 100 g. The amount of Co needed for the SPEELS measurements is about a factor of 10^{10} times smaller, which impressively illustrates the sensitivity of this new technique. INS is known to probe bulk spin waves, and in Ref. 26 the dispersion was measured along the Γ-M direction, i.e., along the other high symmetry direction in the basal plane compared to the SPEELS data. A direct comparison to our data is therefore difficult. The authors mentioned, however, that they could fit the measured dispersion with a dispersion relation obtained from the nearest-neighbor Heisenberg model, as well. Within this model the INS data reveals a value of $JS=19.1\pm0.6$ meV. Comparing this value of JS to values in several other publications in which the spin wave dispersion in Co were measured by INS (typically for smaller wave-vector transfers and along the c axis), the quoted values of JS range from 16.5 to 20.1 meV.[26–28] Considering the two very different methods, INS and SPEELS, and the possible uncertainty introduced by the Heisenberg model, we consider the agreement to the INS data as rather satisfying.

The values of JS obtained from SPEELS measurements within the nearest-neighbor Heisenberg model are, however, typically lower than other values reported in literature from both, BLS and INS measurements. We found the same tendency for our results on fcc Co films as well. One could speculate about possible reasons for this difference. At the high-wave-vectors measured by SPEELS, the surface spin wave energies depend very sensitively on the exchange coupling constant at the topmost layers. We are able to include the "bulk" values for JS measured by other techniques and can still obtain a good agreement to the measured dispersion, if we assume that the value of JS is reduced by approximately $\frac{1}{3}$ at the topmost surface layer.[29] We want to point out, however, that the Heisenberg model itself stands on weak footing for an itinerant electron ferromagnet like Co. The good agreement between the model and the experimentally measured dispersion alone, of course, does not guarantee that the underlying physics is properly taken into account. By SPEELS, spin waves are probed in a thickness and wave vector range not accessible by other techniques. To compare the results of other techniques to our experimental data by connecting the different experimental ranges via the Heisenberg model may lead to large uncertainties.

In Fig. 4 (bottom) the width of the spin wave peaks measured for hcp Co films is shown. The width increases with higher spin wave energies. As already mentioned, we attribute the intrinsic width of the spin wave peak to the finite

lifetime of this excitation. In this case, we can estimate the lifetime of the spin waves to be of the order of tens of femtoseconds only. Thus, the lifetime is only two to three times larger than the precession period of these excitations. Such a strong damping of high-wave-vector spin waves is in line with expectations of recent theoretical calculations, which take into account the full dynamics of spin excitations including the decay of spin waves into Stoner excitations. It has been shown, for example, that the shape of the excitation peak measured with SPEELS on fcc Co agrees rather well with the calculated spectral density of spin excitations.[32] A comparison of the spin wave peak width measured on hcp Co on W(110) to the one measured on fcc Co on Cu(001) (not included in Fig. 4), shows that for hcp Co the width is larger by about 15 meV, though the increase with the wave vector is similar.[5] Different reasons could be responsible for this larger damping. One could expect that the electronic structure and the film quality, as well as the substrate may significantly influence the damping. Since, for high wave vectors, surface spin waves are largely confined in the topmost layers, the influence of the substrate should be rather small for an 8 ML film.[30,31] In addition, we find a very similar spin wave width for 3 and 8 ML Co on W(110), which suggests that the effect of the substrate may not to be the dominating contribution, at least in this case. One might expect a larger damping of the hcp Co films grown W(110) compared to the fcc Co film on Cu(001) because of the substantially larger amount of crystalline imperfections of the former system. Among others a commonly observed lattice defect in this system is a hcp/fcc stacking fault.[13] It was shown that such stacking faults result in laterally extended dislocations.[33] Such areas may provide additional possible decay paths for the spin waves which will (almost) not be present in the nearly perfect fcc Co films on Cu(001).

The large damping observed for the spin waves is, of course, in strong contradiction to the Heisenberg model and to any adiabatic description of spin waves. As has been pointed out by Mills and co-workers, this strong damping may drastically influence the dispersion relation of spin waves.[32] It has also been shown by these authors that the results of their much more sophisticated calculations for both the dispersion relation and the width are very sensitive to the underlying electronic structure. It is our hope that the data presented here will stimulate further theoretical work in this field. Elaborate theoretical descriptions of our results going beyond the adiabatic approximation may provide us with a deeper understanding of the dynamics of high-energy spin waves.

In conclusion, we have presented an experimental investigation of high-wave vector spin waves in 8 ML hcp Co films on W(110) measured by SPEELS. In general, we find very similar spin wave properties in this system compared to fcc Co films on Cu(001). For example, pronounced dispersions are observed that are in agreement with the dispersions for surface spin waves calculated in a nearest-neighbor Heisenberg model for both cases. Using this model, the difference in the measured dispersions of hcp and fcc Co can be explained by the different crystalline directions in the two measurements. The strength of the exchange coupling was found to be similar ($JS \approx 15$ meV) for both crystalline phases. The values of JS also reasonably agree with values measured by other techniques that do not have the pronounced surfaces sensitivity of SPEELS. The spin wave peaks measured by SPEELS have a large intrinsic energy width. This has been predicted by theoretical calculations for such high-wave-vector excitations.[32] It can be explained by the strong damping of these excitations due to the decay into Stoner excitations. In these studies, we were able to follow the spin wave dispersion up to the surface Brillouin zone boundary ($\bar{K} = 1.64$ Å^{-1}) on an 8 ML thick hcp Co film. We measured at least two orders of magnitude higher wave-vector transfers compared to BLS studies. Compared to INS, many orders of magnitude less material is needed. This illustrates the possibilities of SPEELS to measure spin wave excitations with high wave vectors at surfaces and in thin films.

We also find a strong dependence of the measured spin wave intensity on the kinetic energy of the incident electrons which is very similar to what we have observed in fcc Co and in Fe on Cu(001). The origin of this strong dependence is not yet understood.

The authors would like to thank the late Dr. Rüdiger Vollmer, for significant contributions towards this as well as previous work on spin-polarized electron energy loss spectroscopy. The authors would like to acknowledge the help of H. Ibach in designing the experiment. We would also thank D. L. Mills and J. Henk for discussions and D.L. Mills for making results available to us prior to publication.

*Electronic address: markus.etzkorn@epfl.ch

[1] B. Hillebrands and K. Ounadjela, *Spin Dynamics in Confined Magnetic Structures* (Springer-Verlag, Berlin, 2002).
[2] M. Plihal, D. L. Mills, and J. Kirschner, Phys. Rev. Lett. **82**, 2579 (1999).
[3] M. R. Vernoy and H. Hopster, Phys. Rev. B **68**, 132403 (2003).
[4] R. Vollmer, M. Etzkorn, P. S. Anil Kumar, H. Ibach, and J. Kirschner, Phys. Rev. Lett. **91**, 147201 (2003).
[5] R. Vollmer, M. Etzkorn, P. S. Anil Kumar, H. Ibach, and J. Kirschner, J. Magn. Magn. Mater. **272-276**, 2126 (2004).
[6] R. Vollmer, M. Etzkorn, P. S. Anil Kumar, H. Ibach, and J. Kirschner, J. Appl. Phys. **95**, 7435 (2004).
[7] R. Vollmer, M. Etzkorn, P. S. Anil Kumar, H. Ibach, and J. Kirschner, Thin Solid Films **464-465**, 42 (2004).
[8] *Handbook of Chemistry and Physics*, edited by D. R. Lide (CRC Press, Boca Raton, 1999).
[9] R. W. Joyner, J. Rickman, and M. W. Roberts, Surf. Sci. **39**, 445 (1973).
[10] H. Knoppe and E. Bauer, Phys. Rev. B **48**, 1794 (1993).
[11] H. Fritzsche, J. Kohlhepp, and U. Gradmann, Phys. Rev. B **51**, 15933 (1995).
[12] M. Pratzer, H. J. Elmers, and M. Getzlaff, Phys. Rev. B **67**,

153405 (2003).
[13] J. Wiebe, L. Sacharow, A. Wachowiak, G. Bihlmayer, S. Heinze, S. Blügel, M. Morgenstern, and R. Wiesendanger, Phys. Rev. B **70**, 035404 (2004).
[14] H. Ibach, D. Bruchmann, R. Vollmer, M. Etzkorn, P. S. Anil Kumar, and J. Kirschner, Rev. Sci. Instrum. **74**, 4089 (2003).
[15] D. T. Pierce and F. Meier, Phys. Rev. B **13**, 5484 (1976).
[16] P. Drescher *et al.*, Appl. Phys. A **63**, 203 (1996).
[17] C. Herring, *Exchange Interactions among Itinerant Electrons*, Vol. IV of Magnetism, edited by G. T. Rado and H. Suhl (Academic Press, New York, 1966).
[18] S. Y. Savrasov, Phys. Rev. Lett. **81**, 2570 (1998).
[19] J. Hong and D. L. Mills, Phys. Rev. B **61**, R858 (2000).
[20] H. Ibach and D. L. Mills, *Electron Energy Loss Spectroscopy and Surface Vibrations* (Academic Press, New York, 1982).
[21] From our experiments on Co on Cu(001) we estimate a reduction of the measured spin wave intensity by about a factor of 3 when going from $\Delta K_{\|}=1.0$ Å^{-1} to 1.12 Å^{-1}[5].
[22] J. Hong and D. L. Mills, Phys. Rev. B **59**, 13840 (1999).
[23] M. G. Cottam, *Linerar and Nonlinear Spin Waves in Magnetic Films and Superlattices* (World Scientific, Singapore, 1994).
[24] The spin wave dispersion relation for a surface spin wave in an hcp crystal with a (0001) surface along the $\bar{\Gamma}$-$\bar{K}$ direction calculated using the nearest-neighbor Heisenberg model is $E(\Delta K_{\|}) = \frac{16}{3}JS[3-\cos(\Delta K_{\|}a_0-2\cos(\Delta K_{\|}a_0/2)\ ]$. Here, E is the spin wave energy and a_0 is the lattice constant (we take the bulk lattice constant of hcp Co $a_0=2.51$ Å).
[25] X. Liu, M. M. Steiner, R. Sooryakumar, G. A. Prinz, R. F. C. Farrow, and G. Harp, Phys. Rev. B **53**, 12166 (1996).
[26] T. G. Perring, A. D. Taylor, and G. L. Squires, Physica B **213-214**, 348 (1995).
[27] G. Shirane, V. J. Minkiewicz, and R. Nathans, J. Appl. Phys. **39**, 383 (1968).
[28] S. Kraśnicki, A. Wanic, Ž. Dimitrijević, and J. Todorović, Physica (Amsterdam) **37**, 501 (1967).
[29] M. Etzkorn, P. S. Anil Kumar, R. Vollmer, H. Ibach, and J. Kirschner, Surf. Sci. **566-568**, 241 (2004).
[30] R. B. Muniz, A. T. Costa, and D. L. Mills, J. Phys.: Condens. Matter **15**, S495 (2003).
[31] A. T. Costa, R. B. Muniz, and D. L. Mills, Phys. Rev. B **68**, 224435 (2003).
[32] A. T. Costa, R. B. Muniz, and D. L. Mills, Phys. Rev. B **70**, 054406 (2004).
[33] M. Pratzer and H. J. Elmers, Phys. Rev. B **72**, 035460 (2005).